Elasticity of Floppy and Stiff Random Networks

M. Wyart,* H. Liang, A. Kabla,† and L. Mahadevan

School of Engineering and Applied Sciences, Harvard University, 29 Oxford Street, Cambridge, Massachusetts 02138, USA

(Received 27 June 2008; published 19 November 2008)

We study the linear and nonlinear elastic behavior of amorphous systems using a two-dimensional random network of harmonic springs as a model system. A natural characterization of these systems arises in terms of the network coordination (average number of springs per node) relative to that of a marginally rigid network δz: a floppy network has $\delta z < 0$, while a stiff network has $\delta z > 0$. Under the influence of an externally applied load, we observe that the response of both floppy and stiff networks is controlled by the critical point corresponding to the onset of rigidity. We use numerical simulations to compute the exponents which characterize the shear modulus, the heterogeneity of the response, and the network stiffening as a function of δz and derive these theoretically, thus allowing us to predict aspects of the mechanical response of glasses and fibrous networks.

DOI: 10.1103/PhysRevLett.101.215501 PACS numbers: 62.20.de

The mechanics of crystalline solids is a fairly well understood subject owing to the simplicity of the underlying lattice which is periodic. In contrast, an understanding of the mechanics of amorphous solids is complicated by the presence of quenched disorder, often on multiple scales. Two structural properties affecting the elasticity of disordered solids are their coordination and the presence of different types of interactions between the constituents of vastly dissimilar strengths. In the case of weakly coordinated covalent glass such as amorphous selenium, the covalent backbone is floppy; i.e., it is continuously deformable with almost no energy cost, but weak interactions such as van der Waals are responsible for the nonvanishing elastic moduli. On the other hand, in highly coordinated covalent glasses, such as silica, or in amorphous particle assemblies where the main interaction is radial, such as emulsions, metallic glasses, or granular matter, the dominant interaction forms a rigid backbone. In foams and fibrous networks which are made of low-dimensional structures such as filaments and membranes, there is a wide separation of energetic scales between stretching and bending modes. These different materials display a range of curious mechanical responses including strongly heterogeneous elastic responses [1–4] and elastic moduli that can be quite sensitive to the applied stress [1,5]. Despite several theoretical advances [6–10], a unified description of these behaviors remains to be given. Here we study the mechanical response of simple floppy and stiff systems as the coordination is continuously varied and propose such a unifying approach.

We start by recalling Maxwell's criterion for rigidity in a central force network by considering a set of N points in d dimensions, subject to N_c constraints in the form of bonds that connect these points. This network has $Nd - N_c$ effective degrees of freedom [ignoring the $d(d+1)/2$ rigid motions of the entire system] and an average coordination number $z = 2N_c/N$. The system is said to be isostatic when the system is just rigid; i.e., the number of constraints and the number of degrees of freedom are just balanced, so that $Nd = N_c$, and $z = 2d$. When $z < z_c$, the network exhibits collective degrees of freedom with no restoring force; these solutions are called soft modes. For such a network made of harmonic springs at rest of stiffness k, the energy can be written as

$$\delta E = \sum_{\langle ij \rangle} \frac{k}{2} [(\delta \vec{R}_i - \delta \vec{R}_j) \cdot \vec{n}_{ij}]^2 + o(\delta R^2), \qquad (1)$$

where $\vec{n}_{ij}$ is the unit vector going from i to j and $\delta \vec{R}_i$ is the displacement of particles i. Soft modes satisfy $\delta E = 0$ or, equivalently, $(\delta \vec{R}_i - \delta \vec{R}_j) \cdot \vec{n}_{ij} = 0 \ \forall \ ij$. In Fig. 1(a), we show the example of a one-dimensional zigzag structure that straightens without an energy cost until the external load does not couple to the soft modes, i.e., when the latter correspond to node displacements that are orthogonal to the load direction; the system then becomes stiff.

To understand how this simple idea carries over to a floppy network, we created disordered two-dimensional networks with up to 10 000 particles using jammed con-

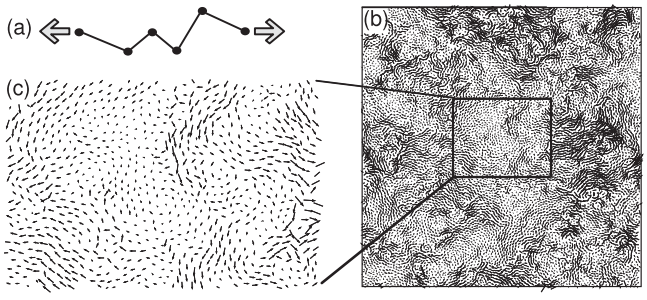

FIG. 1. (a) Stretching a zigzag chain of springs that are freely hinged costs no energy until they are aligned. (b) A random network of 10 000 particles, when subjected to shear, exhibits a heterogeneous response. The coordination is $z = z_c = 4.0$, and the shear strain $\gamma = 0.005$. (c) Zooming in shows the presence of large correlated rotational deformations.

figurations of bidisperse particles [11]. We use periodic boundary conditions on both dimensions. Linear springs initially at rest were then used to connect neighboring particles; starting with $z \approx 5.5 > z_c$, a family of networks with lower coordination is then generated by progressively removing links from the most connected pairs of nodes leading to isotropic networks with low heterogeneity, with a range of spring rest lengths varying by a factor of less than 2. The size of the smallest springs is l and their stiffness k. These networks are different from those studied in rigidity percolation [6] or self-organized networks [7], where the fluctuations in coordination are dominant and can rigidify parts of the system even if $z < z_c$. In addition, to model the presence of weak interactions, we introduce weak springs [of vanishingly small dimensionless stiffness $k_w \equiv \tilde{k}_w/k = 10^{-5}$ except when stated otherwise, and $(\tilde{\cdot})$ designates dimensional quantities] with a number density ρ_w which stabilize the system. We impose a pure shear deformation on the network incrementally and minimize the system energy via a damped molecular dynamics method. The dimensionless shear stress $\sigma \equiv \tilde{\sigma}/k$ is then computed [12]; Figs. 1(b) and 1(c) show the response to shear for $z = 4$ and $\gamma = 0.005$.

In Fig. 2(a), we quantify the elastic properties as a function of parameters and show the existence of three qualitatively different stress-strain relations. For floppy networks with $z - z_c = \delta z < 0$, there is a critical strain γ^* separating a zero stress plateau and a strain-stiffening regime; this critical strain γ^* is a function of the deficit in coordination number δz and follows the scaling law $\gamma^* \sim |\delta z|^\beta$, with $\beta = 1$, over nearly two decades up to $z = 3$ and a strain as large as 40%. For an isostatic system with $\delta z = 0$, the system resists shear deformations nonlinearly as soon as $\gamma \neq 0$; indeed, the stress-strain relation is parabolic $\sigma \sim \gamma^2$, as shown in Fig. 2(c). Finally, for a stiff system with $\delta z > 0$, a linear stress-strain regime can be identified; however, both the value of the dimensionless shear modulus $G \equiv \tilde{G}/k$ and the extent of the linear regime vanish as $\delta z \to 0$, as we discuss quantitatively below.

Since the scaling relations in Figs. 2(b) and 2(c) are reminiscent of a critical point, we look for scaling functions on which all of the stress-strain curves must collapse after a suitable rescaling of the axis. Postulating $G \sim \delta z^\theta$ for $z > z_c$, we write

$$\sigma = G(\delta z)\gamma f_\pm(\gamma/\gamma^*) \equiv |\delta z|^\theta \gamma f_\pm\left(\frac{\gamma}{|\delta z|^\beta}\right), \qquad (2)$$

where the functions f_+ (f_-) characterize the stress-strain relation of stiff (floppy) networks when $\delta z > 0$ ($\delta z < 0$). When the argument of f vanishes, the existence of both a linear and a floppy regime implies that $f_+(x) \to c$, where c is a constant of order one and $f_-(x) \to 0$. For $\gamma > 0$ and $\delta z \to 0$, σ must not vanish. This implies the existence of a power-law form $f(x) \sim x^\chi$ for large x, with $\chi = \theta/\beta$. Previous numerical and empirical studies [3,4,11] show that $\theta = 1$ in two and three dimensions and were justified theoretically [13]. Our numerical results in Fig. 2(b) imply that $\beta = 1$ and Fig. 2(c) implies that $\chi = 1$, in agreement with the relation derived. To directly check the validity of Eq. (2), we rescale the axes of Fig. 2(a) and show the results in Fig. 2(d) vindicating our choice of scaling functions.

Moving beyond the scaling properties of the stress-strain curves, we now consider the structure of the displacement

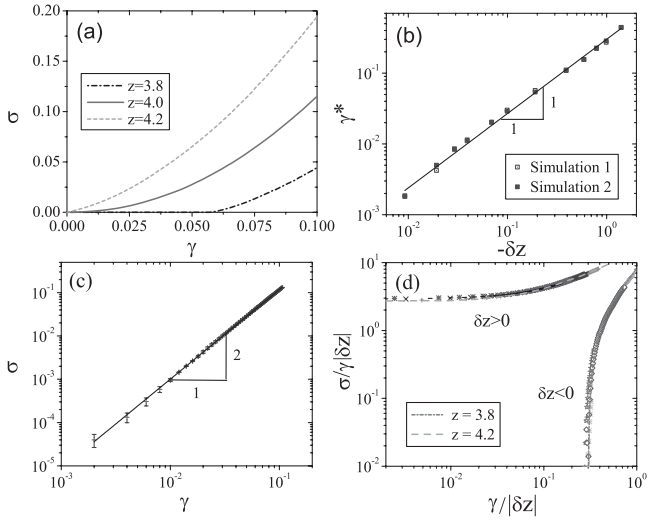

FIG. 2. (a) Dimensionless stress-strain curves for $z = 3.8$, 4.0, and 4.2. (b) Critical strain γ^* vs $\delta z \equiv z - 4$. Each point averages over 2 configurations. (c) Log-log plot of dimensionless stress-strain curve for $z = 4$. (d) Rescaled stress-strain curves for $z = 3.0$, 3.2, 3.4, 3.6, 3.8, 3.9, 3.96, 4.2, 4.4, 4.6, 4.8, and 4.99 show that both floppy and stiff networks can be described in terms of the relative coordination δz.

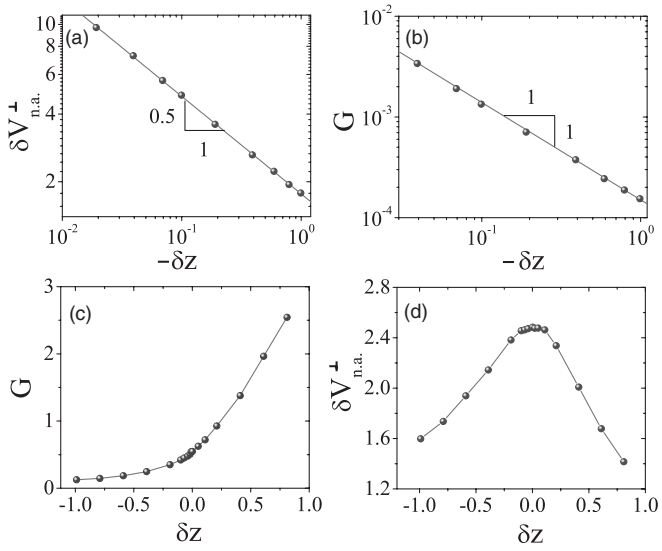

FIG. 3. (a) The relative nonaffine displacement per unit strain as defined in the text $\delta V^\perp_{\text{n.a.}}$ for $\gamma = \gamma^*/10$ and (b) the dimensionless shear modulus G vs $-\delta z$, in the floppy regime, for $k_w = 10^{-5}$. The variation in (c) the dimensionless shear modulus G and (d) $\delta V^\perp_{\text{n.a.}}$ vs $\delta z \in [-1, 1]$, with $k_w = 1/300$, $\rho_w = 4.1$. Note the large particle displacement rate near $\delta z = 0$.

fields shown in Fig. 1(b). The heterogeneity of the response can be characterized by the dimensionless nonaffine displacement field $\{\delta\vec{R}^i_{\text{n.a.}}(\gamma)\}_{i=1\ldots N}$ defined as $\delta\vec{R}^i_{\text{n.a.}} = \vec{R}^i - \vec{R}^i_{a.}$, where $\vec{R}^i$ is the final equilibrated configuration and $\vec{R}^i_{a.}$ is the affine response to a homogeneous strain γ, where all distances are in units of l. We focus on the amplitude of the relative displacement among nearest neighbors $\delta R^{\perp}_{\text{n.a.}} \equiv \langle|\delta\vec{R}^i_{\text{n.a.}} - \delta\vec{R}^j_{\text{n.a.}}|\rangle$, where the average is made on all springs. This is a measure of the rotation of individual springs; the variation in this quantity per unit strain is $\delta V^{\perp}_{\text{n.a.}} \equiv \partial\delta R^{\perp}_{\text{n.a.}}(\gamma)/\partial\gamma$. In Fig. 3(a), we show that for floppy systems $\delta V^{\perp}_{\text{n.a.}} \sim |\delta z|^{\phi}$, with $\phi = -1/2$; i.e., as the floppy network becomes more constrained, larger and larger displacements are required to accommodate a given shear. The network acts as a lever, whose amplification factor diverges as one approaches the onset of rigidity. This scaling has already been observed in assemblies of elastic particles above the rigidity onset ($\delta z > 0$) [4].

We derive this result for $\delta z > 0$. A small affine deformation of amplitude γ causes dimensionless forces $|\delta F\rangle \equiv \{\vec{F}^i\}$ on each node. Assuming for convenience of notation that the stiffnesses and lengths of all spring are equal leads to $\vec{F}^i = \sum_j(\vec{n}_{ij}\cdot\Gamma\cdot\vec{n}_{ij})\vec{n}_{ij}$, where Γ is the corresponding strain tensor and the sum is on all of the neighbors j of i. For a stiff system with $\delta z > 0$, the nonaffine displacement $|\delta R\rangle \equiv \{\delta\vec{R}^i_{\text{n.a.}}\}$, which corresponds to the displacement of the particle along the direction of unbalanced forces, is

$$|\delta R\rangle = M^{-1}|\delta F\rangle = \sum_{\omega}\frac{1}{\omega^2}\langle\delta R(\omega)|\delta F\rangle|\delta R(\omega)\rangle, \quad (3)$$

where M is the dynamical or stiffness matrix and $|\delta R(\omega)\rangle$ is the normalized normal mode of stiffness ω^2. Then the relative displacement between neighboring particles is

$$\delta\vec{R}_{ij} \equiv \delta\vec{R}_i - \delta\vec{R}_j = \sum_{\omega}\frac{1}{\omega^2}\langle\delta R(\omega)|\delta F\rangle\delta\vec{R}_{ij}(\omega). \quad (4)$$

Following the justification of [9], we shall assume that the contribution of the different modes are independent:

$$\langle||\delta\vec{R}_{ij}||^2\rangle = \sum_{\omega}\frac{1}{\omega^4}\langle\delta R(\omega)|\delta F\rangle^2\langle||\delta\vec{R}_{ij}(\omega)||^2\rangle. \quad (5)$$

For weakly coordinated systems, we shall use the results of [14], which show that, above some frequency $\omega^* \sim \delta z$, (i) the density of states $D(\omega)$ does not depend significantly on ω and (ii) modes are not plane-wave-like but very heterogeneous with rapidly decaying spatial correlations; see also [15]. For such modes $\langle||\delta\vec{R}_{ij}(\omega)||^2\rangle \sim \langle||\delta\vec{R}_i(\omega)||^2\rangle = 1/N$, the latter equality stemming from the normalization of the modes. To estimate $\langle\delta R(\omega)|\delta F\rangle^2 = \{\sum_{ij}[\delta\vec{R}_i(\omega) - \delta\vec{R}_j(\omega)]\cdot\vec{n}_{ij}(\vec{n}_{ij}\cdot\Gamma\cdot\vec{n}_{ij})\}^2$, we use the weak spatial correlation of the modes and treat the different terms as independent. Using $\langle(\vec{n}_{ij}\cdot\Gamma\cdot\vec{n}_{ij})^2\rangle \sim \gamma^2$ then leads to

$$\langle\delta R(\omega)|\delta F\rangle^2 \sim \gamma^2\sum_{ij}\{[\delta\vec{R}_i(\omega) - \delta\vec{R}_j(\omega)]\cdot\vec{n}_{ij}\}^2 \sim \gamma^2\omega^2,$$

where $\omega^2 = 1/2\sum_{ij}\{[\delta\vec{R}_i(\omega) - \delta\vec{R}_j(\omega)]\cdot\vec{n}_{ij}\}^2$. Finally, in the large N limit we have $\sum_{\omega}1/N \to \int d\omega D(\omega)$, so that Eq. (5) yields

$$\langle||\delta\vec{R}_{ij}||^2\rangle/\gamma^2 \sim \int d\omega\frac{D(\omega)}{\omega^2} > \int_{\omega>\omega^*} d\omega\frac{1}{\omega^2} \sim \frac{1}{\omega^*} \sim \frac{1}{\delta z}, \quad (6)$$

leading to the relation $\delta R^{\perp}_{\text{n.a.}} \sim ||\delta\vec{R}_{ij}|| \sim \gamma/\sqrt{\delta z}$. Including plane-wave-like modes ($\omega < \omega^*$) in Eq. (6) leads to subdominant corrections.

From this we may deduce the strain at which stiffening occurs. The small applied affine deformation γ causes forces $\vec{F}^i \sim \gamma$, which lead to small nonaffine displacements $\delta\vec{R}^i_{\text{n.a.}} \approx \gamma\vec{u}^i$, where $\vec{u}^i \equiv \lim_{\gamma\to 0}\delta\vec{R}^i_{\text{n.a.}}/\gamma$. Since the linear approximation $\delta\vec{R}^i_{\text{n.a.}} = \gamma\vec{u}^i$ is not exact, there are small residual forces on the nodes, but an iterative perturbative procedure can be used to determine the correction to the leading order result. These residual forces may be estimated following Pythagoras's theorem: the transverse relative displacement at a contact causes a strain and therefore a residual force of the order of $\delta R^{\perp 2}_{\text{n.a.}}(\gamma) \sim \gamma^2\delta z^{2\phi}$. When this quantity becomes larger that $\vec{F}^i \sim \gamma$, the linear approximation breaks down. This occurs for some $\gamma^* \sim \delta z^{\beta} \sim \delta z^{-2\phi}$, yielding the relation $\beta = -2\phi = 1$ observed in our numerical simulations. In other words, the divergence in the displacement rate implies that nonlinearities occur at a very small strain.

The previous argument also yields the scaling form for the dimensionless shear stress G in the floppy regime when weak interactions are not vanishingly small. Indeed, when a shear strain γ is imposed, each weak spring stores a dimensionless energy of order $\delta E \sim k_w\delta V^{\perp 2}_{\text{n.a.}}$, leading to $G \sim \rho_w k_w\delta E/\gamma^2 \sim \rho_w k_w/|\delta z|$ in the floppy regime, as observed in Fig. 3(b). Obviously, this scaling is expected to fail near the rigidity threshold, and we expect a crossover to occur when $G \sim \delta z$ as expected for the backbone of stiff interactions from our earlier scaling arguments. This allows us to define a characteristic coordination scale $u^* \sim \sqrt{\rho_w k_w}$ so that there is an associated critical strain $\gamma^* \sim u^* \sim \sqrt{\rho_w k_w}$ where our two estimates are of the same order. This defines three regimes for the mechanical response as a function of the relative coordination: (i) for $\delta z \ll -u^*$, $G \sim (\rho_w k_w)/|\delta z|$ and $\gamma^* \sim -\delta z$. (ii) For $-u^* \ll \delta z \ll u^*$, $G \sim u^* \sim \sqrt{\rho_w k_w}$ and $\gamma^* \sim u^*$. (iii) For $\delta z \gg u^*$, $G \sim \delta z$ and $\gamma^* \sim \delta z$. Figure 3(c) shows the crossover of the shear modulus as the coordination increases. To confirm this description, we compute $\delta V^{\perp}_{\text{n.a.}}$ for different coordinations, as plotted in Fig. 3(d) for $k_w = 1/300$. Although the ratio of stiffnesses between weak and strong springs is large, the intermediate region is of significant amplitude and vanishes only as the square root of this ratio.

We conclude with a brief discussion of our results and their implications. Using numerical simulations of a weakly coordinated network as an exploratory tool, we have shown that (i) stiff and floppy networks are controlled by the same critical point and (ii) two exponents ϕ and θ, which characterize the amplitude of nonaffine displacements and the shear modulus, respectively, completely characterize the system; all other exponents describing the effects of nonlinearities and the stiffness induced by weak interactions follow from these. Near the rigidity threshold, the amplitude of the nonaffine displacement rapidly increases, and the material response is then characterized by a point on a two-dimensional phase diagram $(\delta z, u^*)$. Note that, although our numerical simulations were carried out in two dimensions, our theoretical arguments apply in three dimensions as well, where we predict the same values for the exponents. In the context of glasses, our model may describe tetrahedral network glasses, such as silica, amorphous silicon, or water, where fluctuations of coordination are rare at reasonable pressures. Such networks, if the joints linking tetrahedra are assumed soft, are marginally rigid [13,16], and the dominant weak interaction rigidifying the system is the energy required to change the angle between two adjacent tetrahedra, whose strength is small for silica and much larger for silicon. Thus, silica is expected to behave effectively as a weakly coordinated network and exhibit large nonaffine displacements, while amorphous silicon should not. In contrast, for chalcogenide glasses where the composition of atoms of different valence can be modified to control rigidity [17], the precise topology of the covalent network near the rigidity threshold is still unsettled [18,19]. Our model is presumably the simplest approximation of such networks and gives a plausible explanation for the observation of a smooth crossover in the elastic moduli near z_c [20]: although other interactions are significantly softer than bending and stretching covalent bonds, their effect is not negligible near z_c due to the lever effect of the backbone and, further, predicts that the nonaffine displacement will be maximum near the rigidity threshold. In solid foams or stiff fiber networks, the different interactions at play (for instance, bending, stretching, and cross-link rigidity) determine the effective coordination. Since bending is a softer mode than stretching, those fibrous systems will be, in general, floppy. Our work yields the simple prediction that the strain γ^* at which the system begins to stiffen and the amplitude of the nonaffine displacement will be anticorrelated and that γ^* will decrease as cross-links are added or fiber length is increased. At a quantitative level, we expect the corresponding exponents to depend on the particular structural properties of the network [8,21]. In particular, (i) if long fibers are present, nonaffine displacements are enhanced, $\delta V_{\mathrm{n.a.}}^{\perp} \sim 1/|\delta z|$ [8], so that nonlinearities arise at a smaller strain, and (ii) if the link size has a broad distribution, small links will effectively act as points of higher coordination, leading to a reduced γ^*. More generally, our study suggests that the amplitude of the nonaffine displacements allows us to classify amorphous solids according to their closeness to criticality.

We thank Ning Xu for providing the jammed configurations, Oskar Hallatschek for discussions, an anonymous referee for detailed constructive comments, and the NSF-Harvard MRSEC for partial support.

*Present address: Janelia Farm Research Campus, 19700 Helix Drive, Ashburn, VA 20147, USA.

†Present address: Engineering Department, Cambridge University, Trumpington Street, Cambridge CB2-1PZ, United Kingdom.

[1] J. Liu, G. H. Koenderink, K. E. Kasza, F. C. MacKintosh, and D. A. Weitz, Phys. Rev. Lett. **98**, 198304 (2007).

[2] F. Leonforte, R. Boissiere, A. Tanguy, J. P. Wittmer, and J.-L. Barrat, Phys. Rev. B **72**, 224206 (2005); **66**, 174205 (2002).

[3] I. Agnolin and J.-N. Roux, Phys. Rev. E **76**, 061304 (2007).

[4] W. G. Ellenbroek, E. K. Somfai, M. van Hecke, and W. van Saarloos, Phys. Rev. Lett. **97**, 258001 (2006).

[5] K. Tanaka, Solid State Commun. **60**, 295 (1986).

[6] Y. Cai and M. F. Thorpe, Phys. Rev. B **40**, 10 535 (1989).

[7] M. F. Thorpe *et al.*, J. Non-Cryst. Solids **266**, 859 (2000).

[8] C. Heussinger and E. Frey, Phys. Rev. Lett. **97**, 105501 (2006).

[9] C. E. Maloney, Phys. Rev. Lett. **97**, 035503 (2006).

[10] B. A. DiDonna and T. C. Lubensky, Phys. Rev. E **72**, 066619 (2005).

[11] C. S O'Hern, L. E. Silbert, A. J. Liu, and S. R. Nagel, Phys. Rev. E **68**, 011306 (2003).

[12] σ is the shear component of the stress tensor $\frac{1}{2V}\sum_{ij}\vec{f}_{ij} \otimes (\vec{R}_j - \vec{R}_i)$, where V and $\vec{f}_{ij}$ are the dimensionless system volume and the contact force in the link ij, respectively, and $\otimes$ is the tensor product.

[13] M. Wyart, Ann. Phys. (Paris) **30**, 1 (2005); arXiv:0806.4653; arXiv:0806.4596.

[14] M. Wyart, L. E. Silbert, S. R. Nagel, and T. A. Witten, Phys. Rev. E **72**, 051306 (2005).

[15] L. E. Silbert, A. J. Liu, and S. R. Nagel, arXiv:0803.2696.

[16] M. T. Dove *et al.*, Mineral Mag. **59**, 629 (1995).

[17] J. C. Phillips, J. Non-Cryst. Solids **43**, 37 (1981).

[18] P. Boolchand, G. Lucovsky, J. C. Phillips, and M. F. Thorpe, Philos. Mag. **85**, 3823 (2005).

[19] K. Tanaka, Phys. Rev. B, **39**, 1270 (1989).

[20] S. Gapochenko and V. Bazakutsa, J. Non-Cryst. Solids **270**, 274 (2000).

[21] D. A. Head, A. J. Levine, and F. C. MacKintosh, Phys. Rev. E **72**, 061914 (2005).